

Charge transport in $\text{Ho}_x\text{Lu}_{1-x}\text{B}_{12}$: Separating Positive and Negative Magnetoresistance in Metals with Magnetic Ions

N.E. Sluchanko^{a,b,*}, A.L. Khoroshilov^{a,b}, M. A. Anisimov^a, A.N. Azarevich^{a,b},
A.V. Bogach^a, V.V. Glushkov^{a,b}, S.V. Demishev^{a,b}, V.N. Krasnorussky^a, V.V.
Voronov^a, N.Yu. Shitsevalova^c, V.B. Filippov^c, A.V. Levchenko^c, G. Pristas^d, S.
Gabani^d, K. Flachbart^d

^a A. M. Prokhorov General Physics Institute, Russian Academy of Sciences, 38 Vavilov str.,
Moscow, 119991 Russia

^b Moscow Institute of Physics and Thechnology, Institutskii per. 9, Dolgoprudnyi, Moscow
Region 141700, Russia

^c I. N. Frantsevich Institute for Problems of Materials Science, National Academy of Sciences
of Ukraine, 3 Krzhizhanovskii str., Kiev, 03680 Ukraine

^d Institute of Experimental Physics of Slovak Academy of Sciences, 47 Watsonova str., 040
01 Košice, Slovak Republic
e-mail: nes@lt.gpi.ru

Abstract

The magnetoresistance (MR) $\Delta\rho/\rho$ of cage-glass compound $\text{Ho}_x\text{Lu}_{1-x}\text{B}_{12}$ with various concentration of magnetic holmium ions ($x \leq 0.5$) has been studied in detail concurrently with magnetization $M(T)$ and Hall effect investigations on high quality single crystals at temperatures 1.9-120 K and in magnetic field up to 80 kOe. The undertaken analysis of $\Delta\rho/\rho$ allows us to conclude that the large negative magnetoresistance (nMR) observed in vicinity of Neel temperature is caused by scattering of charge carriers on magnetic clusters of Ho^{3+} ions, and that these nanosize regions with AF exchange inside may be considered as short range order AF domains. It was shown that the Yosida relation $-\Delta\rho/\rho \sim M^2$ provides an adequate description of the nMR effect for the case of Langevin type behavior of magnetization. Moreover, a reduction of Ho-ion effective magnetic moments in the range $3-9\mu_B$ was found to develop both with temperature lowering and under the increase of holmium content. A phenomenological description of the large positive quadratic contribution $\Delta\rho/\rho \sim \mu_D^2 H^2$ which dominates in $\text{Ho}_x\text{Lu}_{1-x}\text{B}_{12}$ in the intermediate temperature range 20-120 K allows to estimate the drift mobility exponential changes $\mu_D \sim T^{-\alpha}$ with $\alpha=1.3-1.6$ depending on Ho concentration. An even more comprehensive behavior of magnetoresistance has been found in the AF state of $\text{Ho}_x\text{Lu}_{1-x}\text{B}_{12}$ where an additional linear positive component was observed and attributed to charge carriers scattering on the spin density wave (SDW). High precision measurements of $\Delta\rho/\rho = f(H, T)$ have allowed us also to reconstruct the magnetic H - T phase diagram of $\text{Ho}_{0.5}\text{Lu}_{0.5}\text{B}_{12}$ and to resolve its magnetic structure as a superposition of $4f$ (based on localized moments) and $5d$ (based on SDW) components.

Keywords: boron compounds, dodecaborides, magnetoresistance, magnetic clusters, anti-ferromagnet, spin density wave, local susceptibility

I. Introduction

Magnetoresistance (MR) as a property of a material to change the value of its resistivity in external magnetic field was discovered by Lord Kelvin in 1856 [1], but the mechanisms which are responsible both for negative and positive MR effects in various materials are still a subject of

debate [2]-[10]. Over the past two decades a number of materials with large MR, such as organic semiconductors [10, 11], pregraphitic carbon nanofibers, hydrogenated and fluorinated graphene [12]-[14], amorphous Si doped with magnetic rare earth ions [15] and bulk germanium doped by multiply charged impurities [16], SnO₂ (Ref.[17]), silver chalcogenides [4, 18, 19] zero-band-gap Hg_{1-x}Cd_xTe (Ref. [20]), frustrated metallic ferromagnets [21] etc., which are characterized by extreme field sensitivity and/or large values of MR, have been studied in detail, because of their potential for technological applications as e.g. magnetic sensors and/or magnetoresistive reading heads in magnetic recording [22]. Special attention has been paid also to several types of compounds with magnetic *d*- or *f*-ions having "colossal" negative magnetoresistance (CMR) as e.g. manganites [23, 24] and cobaltites [25], double perovskites [26], europium-based hexaborides [27], manganese oxide pyrochlores [3, 28], Cr-based chalcogenide spinels [29, 30], chromium dioxides [31], GdSi (Ref.[32]), MnSi (Ref.[33]), CeB₆ and CeAl₂ (Refs.[34, 35]), Zintl compound Eu₁₄MnBi₁₁ (Ref. [36]) etc., where the MR reaches its largest value near ferro- or antiferromagnetic phase transitions and is quite temperature dependent in this region. Some of the aforementioned compounds are half-metals (metallic for one spin orientation of the carriers while insulators for the other orientation), others are degenerate magnetic semiconductors or magnetic metals. At least during the last decade it became evident that colossal magnetoresistance is not exclusive for manganites and debates are emerging that maybe there is some common explanation for these materials beyond (independent on) various structures and/or interactions which characterize each of them. In fact, various types of imperfections (substitution disorder, vacancies and other lattice defects, electronic, magnetic and structural inhomogeneities, non-stoichiometry, phase separation, etc.) can be found in these compounds [11]-[36]. In particular, in the case of manganites both (i) nanometer scale coexisting magnetic clusters and (ii) disorder-induced phase separation with percolative characteristics between equal-density phases, together with short-range polaron formation are the main factors for the dramatic inhomogeneity resulting into a strong influence of external magnetic field and into appearance of the CMR effect [24]. As a result, it is commonly believed at present that a coexistence of various ordered and disordered phases plays the key role in the CMR effect. Moreover, it is argued that the colossal negative magnetoresistance in compounds with magnetic ions is in fact a Griffiths phase singularity arising in thermodynamic properties at $T_M^{rand} \leq T < T_G$, i.e. between the random transition temperature T_M^{rand} and the "pure" transition temperature T_G (Ref. [37]), and that the vicinity to percolation threshold is the key factor to reach the CMR. In addition, the suppression of short-range static and dynamic polaron correlations in magnetic field is considered as another important component to provide the negative MR effect which dominates in magnetic materials just above T_M .

To shed more light on the origin of negative magnetoresistance observed in strongly correlated electron systems at the vicinity of magnetic phase transitions it is useful to investigate model compounds with a quite simple crystalline and magnetic structure where both different types of disorder and a dispersion of size and number of magnetic clusters can be formed and controlled in the vicinity of magnetic phase transition. As promising materials for the study of negative MR effect we have chosen the *fcc* metallic substitutional solid solutions Ho_xLu_{1-x}B₁₂ with Ho magnetic ions embedded in a rigid covalent boron cage of the dodecaboride lattice. Comprehensive investigations of high-quality single crystals of LuB₁₂ with various boron isotope compositions allowed recently to find a new disordered "cage-glass" phase at liquid nitrogen temperatures [38]-[40]. It was shown [39, 40] that the combination of loosely bound states of rare-earth ions in the rigid boron sub-lattice of RB₁₂ compounds (Fig.1a-c) together with randomly arranged boron vacancies (with a concentration $\sim 1-3\%$) (Fig.1d) leads to a development of lattice instability at intermediate temperatures. As a result, in the range $T < T^* \sim 60$ K metallic R³⁺-ions become

frozen in randomly distributed off-center positions inside truncated B_{24} octahedrons (Fig.1b-d). In case of solid solutions $\text{Ho}_x\text{Lu}_{1-x}\text{B}_{12}$ with magnetic rare earth ions, there is also Lu to Ho substitutional disorder which interferes with the random displacements (static disorder) of R-sites in the metallic cage glass phase.

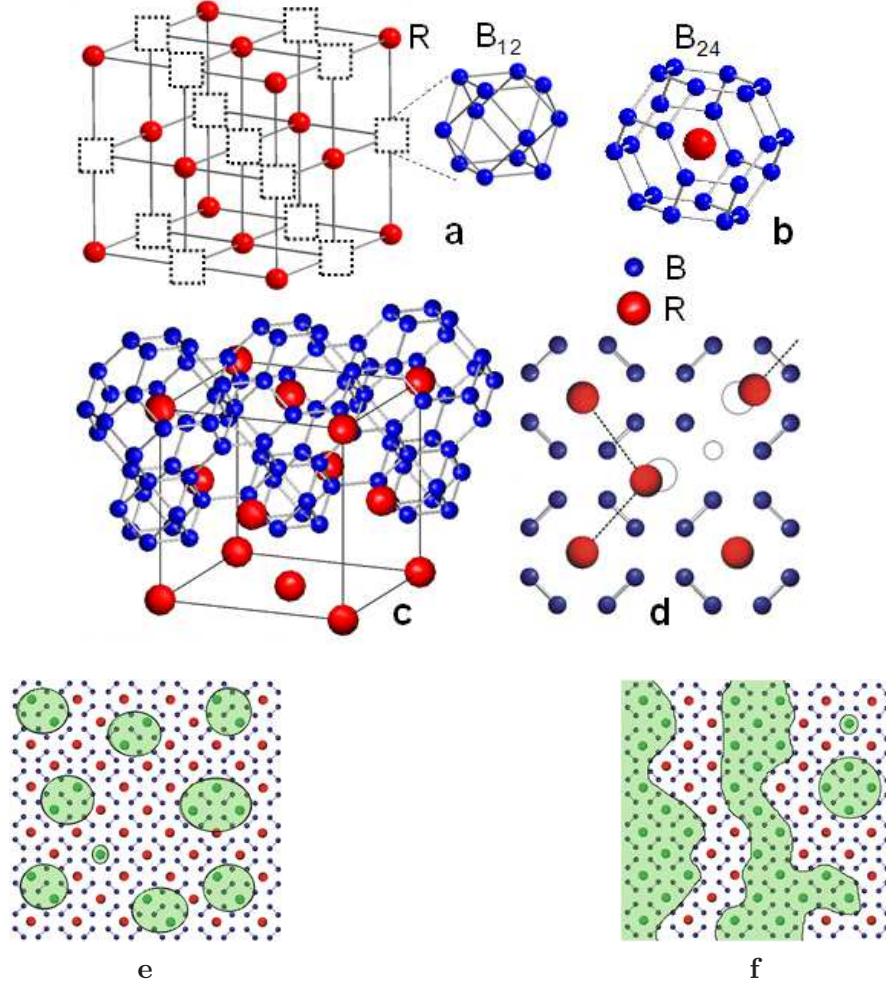


Figure 1. (a) Crystal structure of $\text{Ho}_x\text{Lu}_{1-x}\text{B}_{12}$ compounds. The NaCl-type unit cell is built from R^{3+} ions and B_{12} cubooctahedrons. (b) The first coordination sphere of R^{3+} is arranged as a truncated octahedron B_{24} . The arrangement of R and B atoms along the direction $\langle 110 \rangle$ and in the (110) section is presented in (c) and (d), respectively. For clarity, B_{12} and B_{24} clusters are shown in (c) only along the upper face diagonal of the lattice. A lattice defect (boron vacancy) is shown (small open circle) in (110) section (d). Broken $\text{R}-\text{B}$ bonds in the vicinity of boron vacancy cause displacements of the nearest R^{3+} ions away from the defect by 0.4\AA . As a result, random displacements of the R^{3+} ions, R^{3+} dimers and other small-size rare earth clusters (shown in (d)) appear in RB_{12} matrix. (e) Magnetic clusters of holmium ions in $\text{Ho}_x\text{LuB}_{12}$ solid solutions in the dilute limit $x \leq 0.1$. (f) Formation of infinite magnetic clusters of holmium ions when holmium concentration $x(\text{Ho})$ exceeds the value of the percolation threshold x_C (see the text).

In previous magnetoresistance measurements of the non-magnetic reference compound LuB_{12} and of the antiferromagnetic (AF) HoB_{12} in AF and paramagnetic (P) states a large negative MR effect (of about 30% in magnetic field $H \sim 80$ kOe) was observed in HoB_{12} in the vicinity of AF-P phase transition [41]. Taking into account that holmium to lutetium substitution in $\text{Ho}_x\text{Lu}_{1-x}\text{B}_{12}$ system is accompanied with Neel temperature lowering from $T_N \approx 7.4$ K for $x=1$ to

$T_N \approx 1.9$ K for $x=0.3$ [42, 43] and that at least for $x \leq 0.1$ a paramagnetic ground state is detected in these dodecaborides, it becomes possible to investigate the emergence of the negative MR effect in absence of AF long range order in diluted magnetic compounds with small nanosize magnetic clusters of Ho-ions embedded in the boron matrix (Fig.1e). Moreover, an infinite magnetic cluster of holmium ions is expected to appear when the $x(\text{Ho})$ concentration exceeds the percolation threshold value x_C in the *fcc* lattice (Fig.1f), which is accompanied by AF ground state formation in $\text{Ho}_x\text{Lu}_{1-x}\text{B}_{12}$ in the range $0.2 < x < 0.3$. Thus, the role of different size magnetic clusters during the emergence of large negative MR effect may be investigated in details in vicinity of AF-P phase boundary in these cage-glass metals.

The aim of this work was to perform a comparative study of transverse magnetoresistance both for diluted magnetic ($x=0.01, 0.04, 0.1, 0.15$ and 0.19) and more concentrated antiferromagnetic ($x=0.23, 0.3$ and $x=0.5$, Ref. [42]) $\text{Ho}_x\text{Lu}_{1-x}\text{B}_{12}$ solid solutions in the temperature range 1.9-100 K and in magnetic fields up to 80 kOe. In parallel, we have performed also Hall effect measurements at $H=80$ kOe for $x=0.1$ and $x=0.5$ to compare the drift and Hall mobility of charge carriers, and to clarify the origin of the negative and positive MR components. Additionally, to provide a link between the negative MR and magnetic properties of these model dodecaborides, we have investigated the magnetic susceptibility of $\text{Ho}_x\text{Lu}_{1-x}\text{B}_{12}$ in a wide temperature range 2-300 K at small magnetic field $H \leq 5$ kOe.

II. EXPERIMENTAL DETAILS

In the present study, detailed investigations of resistivity, transverse magnetoresistance and Hall effect of high-quality single crystalline samples of $\text{Ho}_x\text{Lu}_{1-x}\text{B}_{12}$ solid solutions with $x=0.01, 0.04, 0.1, 0.15, 0.19, 0.23, 0.27, 0.3$ and 0.5 were performed in a wide temperature range (1.9-100 K) and in magnetic fields of up to 80 kOe ($\mathbf{H} \parallel \langle 001 \rangle$). Resistivity and Hall resistance were measured by standard DC five probe technique with the orientation of measuring current $\mathbf{I} \parallel \langle 110 \rangle$. The magnetic susceptibility was measured by a commercial SQUID-magnetometer MPMS-5 (Quantum Design). The single crystals used for measurements were grown by vertical crucible-free inductive floating zone melting with multiple re-melting in an inert gas atmosphere on a setup described in detail in [44]. The high accuracy 0.01-0.02 K of temperature control of the sample holder, which was required to perform numerical differentiation of the experimental curves of magnetoresistance $\Delta\rho/\rho=f(H, T_0)$ with respect to magnetic field, was achieved with the help of commercial temperature controller TC 1.5/300 (Cryotel Ltd.) in combination with a thermometer CERNOX 1050 (Lake Shore Cryotronics, Inc.).

III. EXPERIMENTAL RESULTS

IIIa. Resistivity of $\text{Ho}_x\text{Lu}_{1-x}\text{B}_{12}$.

Figure 2 shows the temperature dependences of electrical resistivity $\rho(T)$ of $\text{Ho}_{0.5}\text{Lu}_{0.5}\text{B}_{12}$ crystal measured in various magnetic fields below 40 kOe in a wider vicinity of the antiferromagnetic - paramagnetic (AF-P) transition. The found Neel temperature $T_N \approx 3.45$ K (Fig.2) coincides with a good accuracy with results received in [42, 43]. As can be seen from Fig.2, below T_N the resistivity rises to a maximum upon cooling and then decreases with lowering temperature. This is a common behavior of the magnetic part of $\rho(T)$ in metallic magnets with periodic non-collinear spin structures, as observed e.g. in holmium [45]. With increasing magnetic field the sharp kink at $T_N=3.45$ K is shifted down to 2 K for $H=32.5$ kOe (fig.2a). This matches

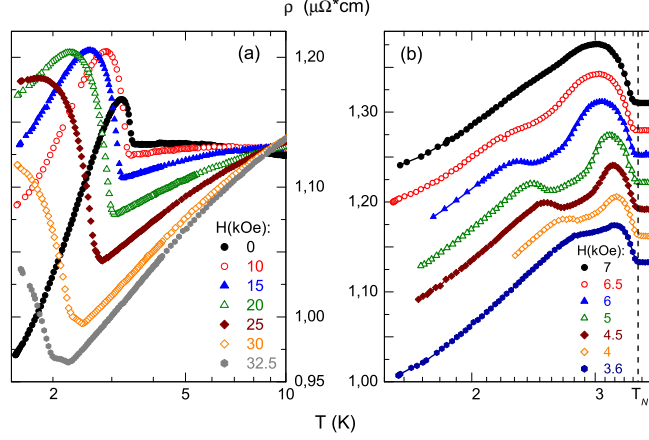


Figure 2. (a-b) The temperature dependences of electrical resistivity $\rho(T)$ of $\text{Ho}_{0.5}\text{Lu}_{0.5}\text{B}_{12}$ compound recorded in magnetic fields $H \leq 40$ kOe. On panel (b) the $\rho(T)$ curves are shifted by a constant value $0.3 \mu\Omega\cdot\text{cm}$ for convenience.

the shift of Neel temperature observed in heat capacity data [42] and the magnetic susceptibility results of this compound [43]. The magnetoresistance ratio $\Delta\rho/\rho = [\rho(H) - \rho(H=0)]/\rho(H=0)$ for $\text{Ho}_{0.5}\text{Lu}_{0.5}\text{B}_{12}$ is -19% (negative MR) at 3.45 K and $H=50$ kOe. Moreover, an additional anomaly in resistivity can be observed just below Neel temperature in low magnetic fields $H < 8$ kOe (fig. 2b) which may be attributed to field dependent spin-orientation magnetic phase transition, similar to that detected inside the AF-phase of HoB_{12} (Ref. [46]).

Figure 3 shows the temperature dependences of resistivity both for diluted ($x=0.1, 0.15$ and 0.19) and concentrated ($x=0.23, 0.27, 0.3$ and 0.5) magnetic $\text{Ho}_x\text{Lu}_{1-x}\text{B}_{12}$ solid solutions in the range 1.9–300 K. For comparison, the $\rho(T)$ curve of the non-magnetic counterpart LuB_{12} (the $4f^{14}$ configuration of Lu ion corresponds to the case of a completely filled $4f$ -shell of the rare earth ion) is also presented in this figure. As can be seen from Fig. 3, all RB_{12} compounds under investigation are good metals, and in absence of external magnetic field their ratio $\rho(300\text{K})/\rho(10\text{K})$ exceeds 10 and reaches a maximum values of about 70 for nonmagnetic LuB_{12} . In the Ho - concentration range $x=0.04-0.19$ the residual resistivity ρ_0 decreases in the range $0.4-0.7 \mu\Omega\cdot\text{cm}$ (see the insert in fig. 3), but between $x=0.23$ and 0.3 ρ_0 exhibits a step-like increase with rising Ho concentration, which is supposed to be a consequence of the emergence of an infinite magnetic cluster (percolation) of Ho-ions (see fig. 1f), although the $\rho(T)$ behavior does not change considerably (fig. 3). At intermediate temperatures resistivity can be described by a power law dependence $\rho(T) \sim T^\alpha$ with exponent α varying in the range between 1.3 and 1.7, depending on holmium content. Fig. 3 displays also the $\rho(T)$ dependencies of both LuB_{12} and solid solutions $\text{Ho}_x\text{Lu}_{1-x}\text{B}_{12}$ with $x=0.1$ in magnetic field of $H=80$ kOe, and for $x=0.3$ at $H=30$ kOe. It is worth to note that when external magnetic field is applied, the $\rho(T, H=80 \text{ kOe})$ dependence of LuB_{12} demonstrates an unconventional increase of resistivity with decreasing temperature below the cage-glass transition at $T^* \sim 60$ K (fig. 3). At the same time, all studied $\text{Ho}_x\text{Lu}_{1-x}\text{B}_{12}$ dodecaborides demonstrate a positive magnetoresistance in strong magnetic field. Taking into account that both negative (fig. 2 – $T < 9\text{K}$, fig. 3a – curve $H=30$ kOe for $x=0.3$) as well as positive (fig. 3b – in $H=80$ kOe) MR effects are observed on high quality single crystals

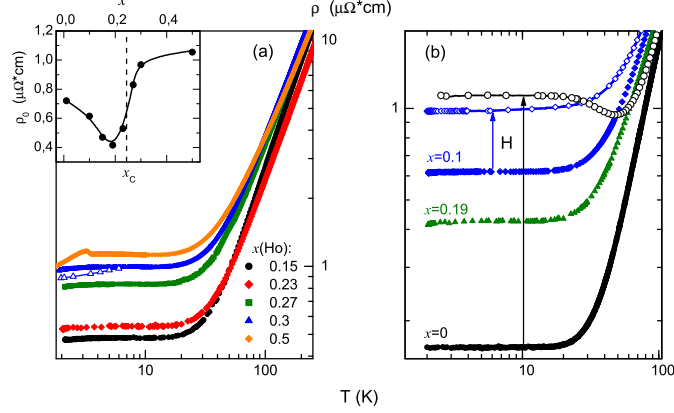


Figure 3. (a-b) The temperature dependences of electrical resistivity $\rho(T)$ of solid solutions $\text{Ho}_x\text{Lu}_{1-x}\text{B}_{12}$ with $x=0, 0.1, 0.15, 0.19, 0.23, 0.3$, and 0.5 . Additionally presented are data for magnetic fields $H=30$ kOe ($x=0.3$, labeled by \triangle symbols on panel (a)) and $H=80$ kOe ($x=0, 0.1$, labeled by \circ, \diamond symbols on panel (b)) are presented. The inset in panel (a) shows the residual resistivity ρ_0 versus the holmium concentration x (see the text).

of $\text{Ho}_x\text{Lu}_{1-x}\text{B}_{12}$, it appears to be important to measure in detail the magnetic field dependencies $\rho(H, T_0)$ in a wide range of temperatures, to separate and classify the magnetoresistance contributions in these magnetic solid solutions with various holmium content.

IIIb. Magnetoresistance of $\text{Ho}_x\text{Lu}_{1-x}\text{B}_{12}$.

Results of MR investigations of $\text{Ho}_x\text{Lu}_{1-x}\text{B}_{12}$ solid solutions with a Ho content $x=0.01, 0.1, 0.3$ and 0.5 are shown in figs.4a, 5a-b, 5c-d and 6a-d, correspondingly. As can be seen from fig.4a, in case of the diluted magnetic solid solution $\text{Ho}_{0.01}\text{Lu}_{0.99}\text{B}_{12}$ the magnetoresistance is positive anywhere and demonstrates a strong increase without a tendency to saturation in high magnetic fields up to 80 kOe. With increase of Ho content in the range $x=0.1-0.5$ the aforementioned positive MR effect dominates in the range of intermediate temperatures $T>20$ K (see figs.5a, 5c, 6a for $x=0.1, 0.3$ and 0.5 , correspondingly), but below 20 K an emergence of a negative contribution may be observed on $\Delta\rho/\rho(H)$ curves, even for $x=0.1$ (fig.5b). At higher Ho concentration, in the range of $x=0.19-0.5$, a pronounced negative minimum appears on MR *vs* magnetic field dependences at liquid helium temperatures (see fig.7 and also figs.5d and 6b) and its amplitude and location are strongly dependent on x . Indeed, the amplitude of negative MR increases essentially in the range $x=0.15-0.5$ (fig.7) where the position of MR minimum changes from $H_{min}^{MR}(x=0.15)\sim 16$ kOe to $H_{min}^{MR}(x=0.5)\sim 51$ kOe (see also figs.5d and 6b-c). For comparison, a negative transverse MR with a large amplitude ($\sim 20-30\%$) was observed previously [41] in the paramagnetic phase of HoB_{12} at temperatures 7.5-15 K. Moreover, the minimum value of negative magnetoresistance in HoB_{12} is expected to be observed in magnetic fields above 80 kOe [41].

The AF-P transition in $\text{Ho}_{0.5}\text{Lu}_{0.5}\text{B}_{12}$ which is, depending on field, observed in the temperature range 1.9-3.5 K, is accompanied by the appearance of an additional positive antiferromagnetic MR contribution (see fig.2 and fig.6c,d) which becomes fully suppressed by external magnetic field when H reaches the critical values $H_N(T_N)$ on the AF-P phase boundary (fig.6d).

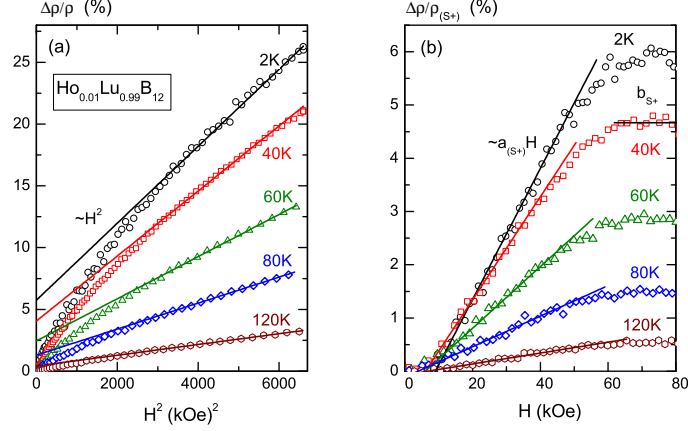


Figure 4. The field dependences of (a) magnetoresistance in coordinates $\Delta\rho(H)/\rho=f(H^2, T_0)$ and (b) $\Delta\rho(H)/\rho_{(S+)}$ the positive MR component of $\text{Ho}_{0.01}\text{Lu}_{0.99}\text{B}_{12}$ compound. The solid lines represent the (a) quadratic asymptotic $\sim H^2$, (b) linear $a_{(S+)}H$ and saturated $b_{(S+)}$ contributions to MR (see the text).

This additional positive MR component can be attributed to charge carrier scattering on the magnetic structure in the AF phase of $\text{Ho}_{0.5}\text{Lu}_{0.5}\text{B}_{12}$. A similar positive magnetoresistance was observed previously in the AF phases of HoB_{12} , ErB_{12} and TmB_{12} dodecaborides [41] and in antiferromagnetic solid solutions $\text{Tm}_{1-x}\text{Yb}_x\text{B}_{12}$ with $x \leq 0.1$ (Ref.[47]). The mechanism which is responsible for this effect will be discussed below.

IIIc. Hall effect and magnetic susceptibility.

Fig.8a displays results of Hall effect measurements that have been carried out simultaneously with magnetoresistance on several crystals of $\text{Ho}_x\text{Lu}_{1-x}\text{B}_{12}$ at magnetic field $H=80$ kOe. A pronounced increase (by 15-25%) of the amplitude of negative Hall coefficient is observed with temperature lowering in the range above the cage-glass transition $T^* \sim 60$ K for all studied Ho contents $x=0.1$ and 0.5 (fig.8a). Then, a moderate decrease of the absolute values of $R_H(T)$ can be observed with temperature lowering below T^* for $\text{Ho}_x\text{Lu}_{1-x}\text{B}_{12}$ compound with $x=0.1$ (fig.8a). But on the contrary, for the most concentrated magnetic dodecaboride with $x=0.5$ a moderate elevation of the negative $R_H(T)$ is observed at $T < T^*$ with a smooth maximum at $T_{max} \sim 25$ K. A similar strong field maximum of negative Hall coefficient was found at 20 K in [48] for HoB_{12} .

The magnetic susceptibility $\chi(T)$ dependencies received in the present study in small magnetic fields $H=0.1$ kOe (for $x=0.1, 0.3$ and 0.5) and in $H=5$ kOe (for $x=0.01$) at temperatures in the range 2-300 K are shown in fig.8b. The $\chi(T)$ dependences demonstrate a paramagnetic Curie-Weiss type behavior, and for $\text{Ho}_x\text{Lu}_{1-x}\text{B}_{12}$ solid solution with $x=0.5$ the AF-P phase transition is observed at $T_N \approx 3.45$ K (fig.8b).

In the further analysis and discussion of these results it will be shown that it is possible to separate and classify the aforementioned positive and negative contributions to magnetoresistance. Moreover, the developed approach will demonstrate that the MR components may be estimated quantitatively and that parameters extracted from the data will allow to describe both the temperature dependence of drift mobility and the characteristics of nanosize magnetic

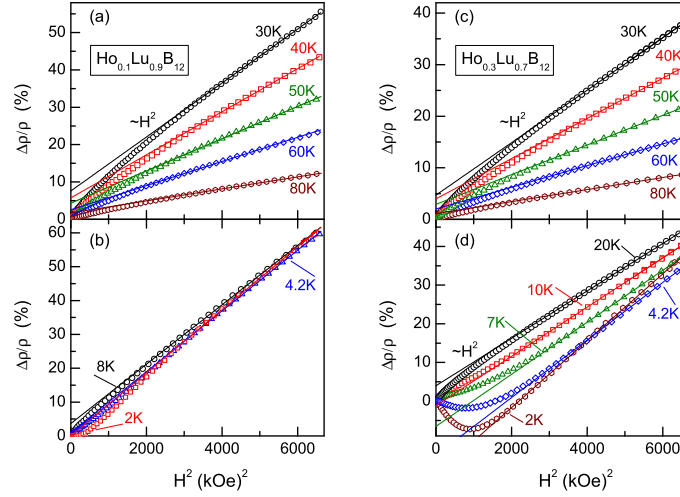


Figure 5. The field dependences of magnetoresistance in coordinates $\Delta\rho(H)/\rho=f(H^2, T_0)$ of (a-b) $\text{Ho}_{0.1}\text{Lu}_{0.9}\text{B}_{12}$ and of (c-d) $\text{Ho}_{0.3}\text{Lu}_{0.7}\text{B}_{12}$ solid solutions. The solid lines in (a-d) represent the quadratic asymptotic $\sim H^2$.

clusters (domains with AF-type short range order) which are composed from interconnected Ho^{3+} -ions embedded in the rigid covalent cage of boron atoms.

IV. DISCUSSION

To separate and characterize analytically the large negative magnetoresistance effect observed in vicinity of AF-P transition in $\text{Ho}_{0.5}\text{Lu}_{0.5}\text{B}_{12}$ (fig.2) it is first necessary to analyze several positive MR components which are dominant (i) at intermediate temperatures 20-100 K and (ii) in the antiferromagnetic state of $\text{Ho}_x\text{Lu}_{1-x}\text{B}_{12}$ compounds. The most effective approach here is based on investigations of the positive MR in the paramagnetic state of diluted $\text{Ho}_x\text{Lu}_{1-x}\text{B}_{12}$ solid solutions (with a small concentration of magnetic impurities $x=0.01$ and 0.1). From the side of percolation threshold (see inset in fig.3a), for $x=0.3$ and 0.5, a large negative MR component appears at low temperatures ($T_N \leq T \leq 10$ K) versus the positive MR background, and these terms should be analyzed in combination with each other. In the approximation of several additive processes in the scattering of charge carriers in $\text{Ho}_x\text{Lu}_{1-x}\text{B}_{12}$, we will gradually develop a phenomenological approach to separate of the MR contributions, and then propose the interpretation of the large negative magnetoresistance. We will demonstrate that large negative MR effect may be explained by scattering of charge carriers on the small size magnetic clusters of Ho-ions, and the Yosida-type relationship $-\Delta\rho/\rho \sim L^2(H/T)$ (L - Langevin function) will provide us with a good quality approximation of the negative magnetoresistance behavior. Simultaneously, the analysis of MR in the AF phase will allow us to conclude in favor of a combination of $5d$ and $4f$ - components which interplay with each other in the formation of the complicated magnetic structure of $\text{Ho}_{0.5}\text{Lu}_{0.5}\text{B}_{12}$.

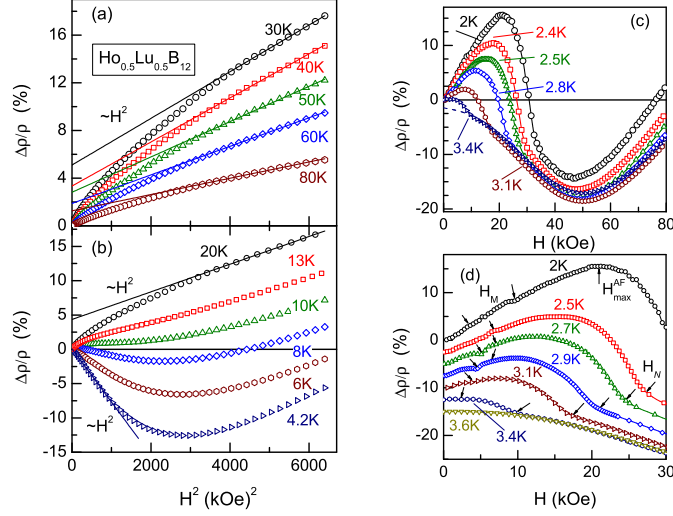


Figure 6. The field dependences of magnetoresistance in coordinates (a-b) $\Delta\rho(H)/\rho=f(H^2, T_0)$ and (c, d) $\Delta\rho(H)/\rho=f(H, T_0)$ of $\text{Ho}_{0.5}\text{Lu}_{0.5}\text{B}_{12}$ compound. The solid lines in (a-b) represent the quadratic asymptotic $\sim H^2$. The $\Delta\rho(H)/\rho$ curves in (d) are shifted by a constant value $\Delta\rho/\rho=2.5\%$ for convenience. Arrows in (d) indicate the magnetic phase transitions (see the text).

IVa. Positive magnetoresistance in the paramagnetic phase of $\text{Ho}_x\text{Lu}_{1-x}\text{B}_{12}$.

Both the MR data presented in coordinates $\Delta\rho/\rho=f(H^2, T_0)$ (see solid lines in figs.4a, 5a, c and 6a, b) and their numerical derivatives ($d(\Delta\rho/\rho)/dH=f(H, T_0)$) (see Fig.S1 in the Supplementary Information) reveal that the positive magnetoresistance observed at intermediate temperatures in high magnetic fields 50-80 kOe follows the quadratic field dependence $\Delta\rho/\rho_{(m+)}=\mu_D^2 H^2$, where from conventional approach the parameter μ_D may be considered as the reduced drift mobility of charge carriers. Additionally to this dominant quadratic term $\Delta\rho/\rho_{(m+)}$, there is another positive component $\Delta\rho/\rho_{(s+)}$ detected in a moderate magnetic fields. This second positive MR contribution may be singled out at intermediate temperatures by subtracting the strong field term $\Delta\rho/\rho_{(m+)}=\mu_D^2 H^2$ from the observed experimental $\Delta\rho/\rho(H)$ dependence. The final $\Delta\rho/\rho_{(s+)}$ is shown, for example, in figs.4b and 9a, b for holmium content $x=0.01$ and 0.1, respectively. It can be seen from these figures that the second term is negligible in small magnetic fields $H\leq 5$ kOe, but it demonstrates an approximately linear field dependence $\Delta\rho/\rho_{(s+)}\sim a_{(s+)}H$ in the range of 10-40 kOe. Then it saturates at high magnetic fields (figs.4b, 9a) and its amplitude $b_{(s+)}$ does not exceed 9% at $T>7$ K for all $\text{Ho}_x\text{Lu}_{1-x}\text{B}_{12}$ crystals studied. Moreover, in case of the diluted magnetic system $\text{Ho}_{0.01}\text{Lu}_{0.99}\text{B}_{12}$ the magnetoresistance exhibits only these two positive contributions both at intermediate and liquid helium temperatures (fig.4b). In the absence of the negative MR the analysis of two positive terms $\Delta\rho/\rho_{(m+)}$ and $\Delta\rho/\rho_{(s+)}$ allows to deduce the temperature dependences of the above-mentioned coefficients μ_D , $a_{(s+)}$ and $b_{(s+)}$ for $x=0.01$, and also for $x\geq 0.1$ in the range $T>10$ K. The resulting $\mu_D(T)$ dependence acquired directly from data of figs.4-6 and fig.9 is shown on fig.10a. Additionally, fig.10b shows for comparison the high field Hall mobility $\mu_H(T)=R_H(T)/\rho(T)$ for $\text{Ho}_x\text{Lu}_{1-x}\text{B}_{12}$ with $x=0.1$ and 0.5. It can be seen that the behavior of reduced drift μ_D and Hall μ_H mobility at $H=80$ kOe is similar to each other, and that exponents α_D and α_H in dependences

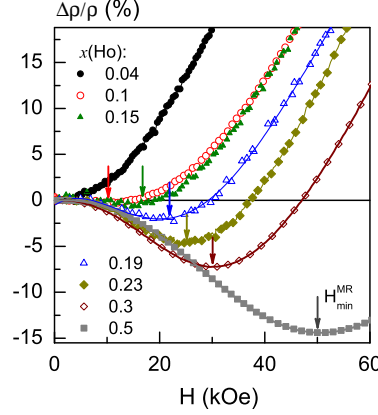


Figure 7. The field dependences of magnetoresistance of solid solutions $\text{Ho}_x\text{Lu}_{1-x}\text{B}_{12}$ with $x=0.04, 0.1, 0.15, 0.19, 0.23, 0.3$ ($T_0=2$ K) and 0.5 ($T_0=3.6$ K). The arrows indicate the positions of pronounced negative minima on MR data.

$\mu_D(T) \sim T^{-\alpha_D}$ and $\mu_H(T) \sim T^{-\alpha_H}$ obtained at intermediate temperatures $T \geq T^* \sim 60$ K are about equal in studied compounds ($\alpha_D(x=0.1) \approx \alpha_H(x=0.1) \approx 1.6-1.7$ and $\alpha_D(x=0.5) \approx \alpha_H(x=0.5) \approx 1.3$, see fig.10). The deduced temperature dependences of coefficient $a_{(s+)}$ and the saturation value $b_{(s+)}$ of the $\Delta\rho/\rho_{(s+)}$ contribution of all compounds (see fig.S2 in the SI) are also similar and connect the slope of the linear increase of MR with the amplitude of the second positive MR component of $\text{Ho}_x\text{Lu}_{1-x}\text{B}_{12}$ solid solutions.

IVb. Negative magnetoresistance in the paramagnetic phase of $\text{Ho}_x\text{Lu}_{1-x}\text{B}_{12}$.

Apart from looking for the physical meaning of the second $\Delta\rho/\rho_{(s+)}$ component, it should be stressed that the simple phenomenological procedure applied above for evaluating the positive MR may be developed successfully also to separate the negative magnetoresistance observed for $\text{Ho}_x\text{Lu}_{1-x}\text{B}_{12}$ with $x \geq 0.1$ at low temperatures. Indeed, on the contrary to the dilute compound with $x=0.01$ where the only two positive MR components with coefficients μ_D and $a_{(s+)}$, $b_{(s+)}$ have been observed in a wide temperature range 1.9–120 K (see fig.10a and fig.S2), for magnetic dodecaborides $\text{Ho}_x\text{Lu}_{1-x}\text{B}_{12}$ with $x \geq 0.1$ the emergence of additional negative magnetoresistance is evident at low temperatures $T < 10$ K, and its amplitude increases dramatically with temperature lowering (see figs.9c and 11a, b). Moreover, in $\text{Ho}_x\text{Lu}_{1-x}\text{B}_{12}$ solid solutions the increase of Ho content is accompanied by a strong increase of the negative MR contribution, e.g. between $\Delta\rho/\rho_{(-)}(x=0.1) \sim 3$ % (fig.9c) and $\Delta\rho/\rho_{(-)}(x=0.5) \sim 30$ % (fig.11b). A comparative analysis of data presented in figs.9c and 11 allows to conclude that (i) at low magnetic field the negative MR follows a quadratic dependence $-\Delta\rho/\rho_{(-)} \sim H^2$ and (ii) that the $\Delta\rho/\rho_{(-)}$ term demonstrates also a tendency to saturation in high magnetic fields. It should be mentioned that such kind of behavior of $\Delta\rho/\rho_{(-)}$ is well-known both for manganites [49], non-magnetic and AF heavy fermion compounds like CeCu_6 , CeAl_3 [50] and CeAl_2 , CeB_6 [34, 51], AF metal GdSi [32], etc. Recently this effect has been observed also in dodecaborides HoB_{12} , ErB_{12} and TmB_{12} [41] and hexaborides PrB_6 , NdB_6 and GdB_6 [52, 53], and it was analyzed successfully within the framework of Yosida approach [54] based on s - d exchange model. This model describes the scattering of charge carriers on localized magnetic moments (LMM) by the relationship between

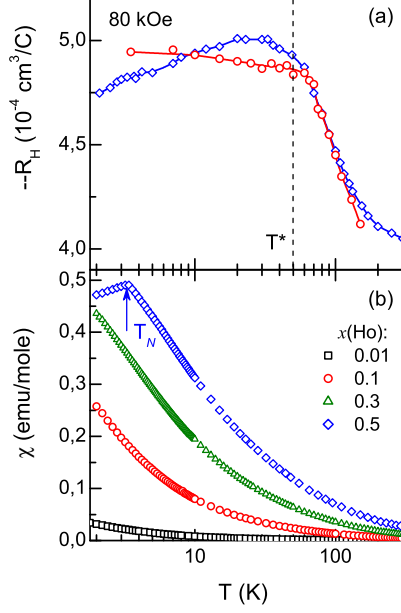


Figure 8. The temperature dependences of (a) negative Hall coefficient $-R_H(T)$ and (b) magnetic susceptibility $\chi(T)$ of solid solutions $\text{Ho}_x\text{Lu}_{1-x}\text{B}_{12}$ with $x=0.01, 0.1, 0.3$ and 0.5 (symbols $\square, \circ, \triangle, \diamond$, respectively).

negative MR and local magnetization \mathbf{M}_{loc}

$$-\Delta\rho/\rho_{(-)} \sim M_{loc}^2. \quad (1)$$

In small magnetic fields, where the linear dependence $\mathbf{M}_{loc} \sim \chi_{loc} \mathbf{H}$ is valid, the relationship (1) allows to explain a simple quadratic field dependence of negative magnetoresistance. Moreover, it was shown in [50]-[53] that the behavior of local magnetic susceptibility $\chi_{loc}(T)$ may be detected directly from the study of the $\Delta\rho/\rho_{(-)}$ term. The emergence of strong negative MR in heavy fermion compounds was attributed [34, 50, 51] to a formation of spin-polaron resonance in the electron density of states (DOS) at E_F , which appears in systems with strong local $4f$ - $5d$ spin fluctuations. Simultaneous polarization of R^{3+} magnetic moments of rare earth ions and of the spins of conduction electrons in external magnetic field destroys the DOS resonance and prevents the on-site spin-flip scattering.

Taking into account the formation of nanosize magnetic clusters of holmium ions in the dodecaboride matrix (see fig.1e, f), it is natural to expect that the Langevin function $L(\alpha) = \coth(\alpha) - 1/\alpha$ (where $\alpha = \mu_{eff}H/k_B T$, k_B is the Boltzmann constant and μ_{eff} the effective magnetic moment of the magnetic nanodomains) should provide an appropriate approximation of the local magnetization behavior. As a result, the sum of three terms $\Delta\rho/\rho_{(m+)} = \mu_D^2 H^2$, $\Delta\rho/\rho_{(s+)} = (a_{(s+)}H; b_{(s+)})$ and $\Delta\rho/\rho_{(-)} = kL^2(\alpha)$ was taken to fit the magnetoresistance at $T < 10$ K in the paramagnetic phase of $\text{Ho}_x\text{Lu}_{1-x}\text{B}_{12}$ solid solutions. In the first step of the procedure the coefficient μ_D was received directly from the approximation of high field experimental data $\Delta\rho/\rho(H, T_0)$ (see e.g. figs.5b, d and 6a). Parameters $a_{(s+)}(T)$, $b_{(s+)}(T)$ and $\mu_{eff}(T)$ have been deduced from the analysis of residual MR data analysis. For example, figures 12a and 12b show the received contributions to magnetoresistance- $\mu_D^2 H^2$, $\Delta\rho/\rho_{(s+)}$ and $kL^2(H/T_0)$ simultaneously with the

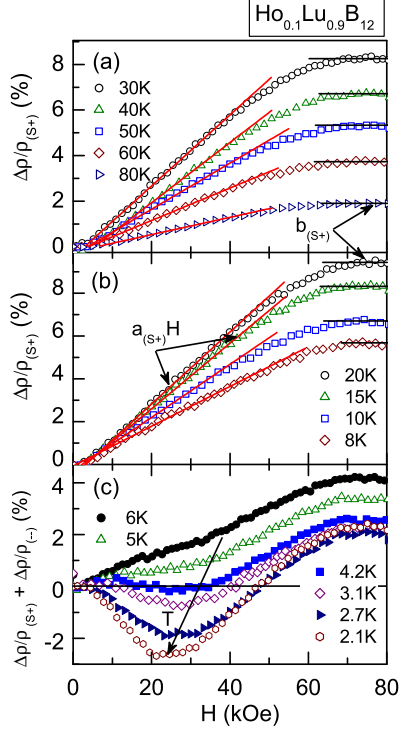


Figure 9. The field dependences of (a-b) $\Delta\rho/\rho_{(s+)}$ and (c) $(\Delta\rho/\rho_{(s+)} + \Delta\rho/\rho_{(-)})$ contributions to MR of $\text{Ho}_{0.1}\text{Lu}_{0.9}\text{B}_{12}$ compound. The solid lines correspond to the positive linear $a_{(s+)}H$ (red) and saturated $b_{(s+)}$ (black) components of MR term $\Delta\rho/\rho_{(s+)}$, respectively.

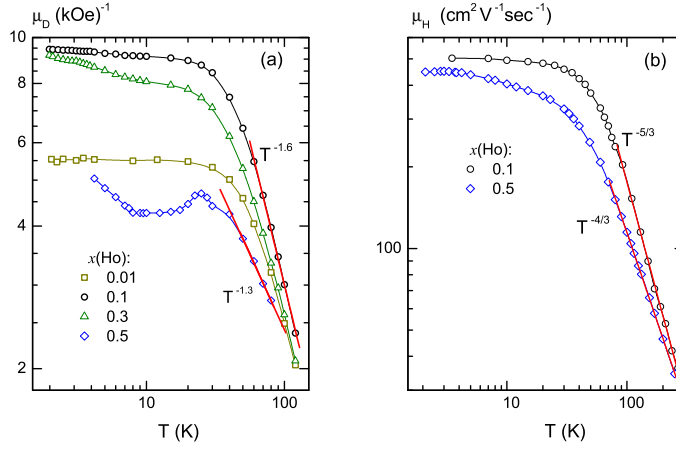


Figure 10. The temperature dependences of (a) the reduced drift mobility of charge carriers $\mu_D(T)$ and (b) Hall mobility $\mu_H(T) = R_H(T)/\rho(T)$ of solid solutions $\text{Ho}_x\text{Lu}_{1-x}\text{B}_{12}$ with $x=0.01, 0.1, 0.3$ and 0.5 (symbols $\square, \circ, \triangle, \diamond$, respectively). The solid lines on both panels represent the data approximation by the power law $\mu \sim T^{-\alpha}$ (see the text).

experimental curves of $\Delta\rho/\rho(H, T_0)$ recorded at $T \sim 2$ K for $x=0.1$ and $x=0.3$, respectively.

Parameters $\mu_{eff}(T, x)$ and $\chi_{loc}^{-1}(T, x_0)$ obtained in the framework of this approach are presented in figs.13 and 14a, correspondingly. For comparison, panel b of fig.14 displays also reciprocal bulk magnetic susceptibility data $\chi^{-1}(T, x_0)$ recorded for the same $\text{Ho}_x\text{Lu}_{1-x}\text{B}_{12}$ crystals. It is worth to note that the reduced local susceptibility $\chi_{loc}(T, x_0)=1/H \cdot (d(-\Delta\rho/\rho)/dH)^{-1/2}$ was deduced directly from small field ($H < 5$ kOe) MR data $\Delta\rho/\rho_{exper} - \Delta\rho/\rho_{(m+)}$, and the parameter $\mu_{eff}(T, x)$ was independently determined by fitting of the sum $\Delta\rho/\rho_{(s+)} + \Delta\rho/\rho_{(-)}$ (see figs.9c, 11a,b) in two magnetic field ranges 10-40 kOe and 60-80 kOe.

For the system with nanosize magnetic clusters arranged from the holmium ions (see fig.1e,f) it is natural to expect a noticeable reduction of μ_{eff} values in comparison with Ho^{3+} magnetic moment $\mu(\text{Ho}^{3+})=10.6 \mu_B$. Indeed, these small size clusters with AF exchange interaction inside them may be considered as nanoscale magnetic domains with AF short range order. In these terms the small size clusters of Ho^{3+} ions with reduced LMM values should be treated as classical magnetic moments with effective moment μ_{eff} whose magnetization is described by the Langevin function $L(\alpha)=cth(\alpha) - 1/\alpha$ (where $\alpha=\mu_{eff}H/k_B T$). A decrease of μ_{eff} is observed in this study both (i) with the temperature lowering (fig.13a) and (ii) with the increase in Ho content (fig.13b) in $\text{Ho}_x\text{Lu}_{1-x}\text{B}_{12}$ solid solutions. Thus, the AF short range order formation can be considered as the most adequate interpretation of the effective moment reduction. The Kondo mechanism of charge carriers scattering cannot be responsible for the negative MR effect in Ho-based dodecaborides, as Ho^{3+} ($4f^{10}$ configuration, Γ_{51} triplet ground state) is not a Kondo-ion. Moreover, the analysis of magnetoresistance of HoB_{12} , ErB_{12} and TmB_{12} undertaken in [41] allows concluding that both spin-polaron and short range order effects are responsible for the appearance of negative magnetoresistance in these dodecaborides. So, the reduction of $\mu_{eff}(T)$ (fig.13a) and $\mu_{eff}(x)$ (fig.13b) in paramagnetic state of these cage-glass compounds with nanosize magnetic clusters may be attributed directly to the extension of AF domains in the RB_{12} matrix. Moreover, following to the developed approach it becomes possible to interpret also the violation of Curie-Weiss law $\chi(T) \sim \mu_{eff}^2/(T - \theta_p)$ observed for all three $\chi_{loc}(T)$ curves (fig.14a, right axis). In this way, taking into account the strong reduction of μ_{eff} with temperature lowering (fig.13a) one has to analyze the product $\chi_{loc}^{-1}(T) \cdot \mu_{eff}^2(T)$ which is expected to follow the Curie-Weiss relation. And indeed, a linear temperature dependence of the product $\chi_{loc}^{-1} \cdot \mu_{eff}^2$ is observed for $\text{Ho}_x\text{Lu}_{1-x}\text{B}_{12}$ crystals with negative MR - $x=0.1, 0.3$ and 0.5 (see fig.14a, left axis). Finally, it should be stressed that for concentrated holmium compounds with $x=0.3$ and $x=0.5$ we have obtained almost equal values of $\chi_{loc}^{-1}(T)$ (fig.14a) and similar values of $\mu_{eff}(T)$ (fig.13a). These results allow us to conclude that these finite size antiferromagnetic nanodomains are responsible both for the spin-flip scattering as well as for the appearance of negative MR in the magnetic dodecaborides.

IVc. Magnetic phase diagram and MR contributions in the AF state of $\text{Ho}_{0.5}\text{Lu}_{0.5}\text{B}_{12}$.

As it was mentioned above, the MR effect in the AF phase of $\text{Ho}_x\text{Lu}_{1-x}\text{B}_{12}$ is quite different from that observed in the paramagnetic state. Indeed, at temperatures $T < T_N$ new large positive magnetoresistance component becomes dominant in moderate magnetic fields, but, in the range $H_{max}^{AF} < H < H_N$ a strong MR decrease can be seen (fig.6c,d). To estimate quantitatively the amplitude of the positive $\Delta\rho/\rho(\text{AF})$ term observed in the AF phase we have used an extrapolation of the sum of paramagnetic contributions observed in the P phase in magnetic fields $H < H_N$ (see fig.6c), then the $\Delta\rho/\rho(\text{AF})$ part can be deduced by subtracting this paramagnetic background from experimental MR data. The obtained AF contribution to MR in $\text{Ho}_{0.5}\text{Lu}_{0.5}\text{B}_{12}$ is shown in

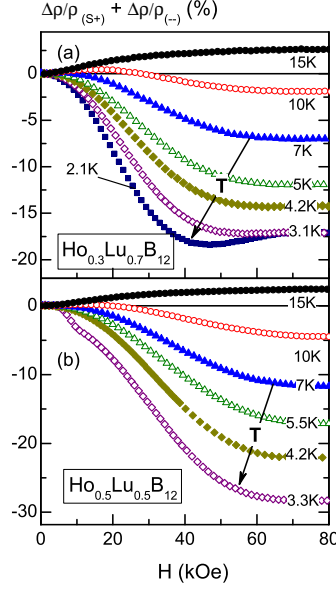


Figure 11. The field dependences of $\Delta\rho/\rho_{(S+)} + \Delta\rho/\rho_{(-)}$ contribution to MR (see text) for (a) $\text{Ho}_{0.3}\text{Lu}_{0.7}\text{B}_{12}$ and (b) $\text{Ho}_{0.5}\text{Lu}_{0.5}\text{B}_{12}$ compounds.

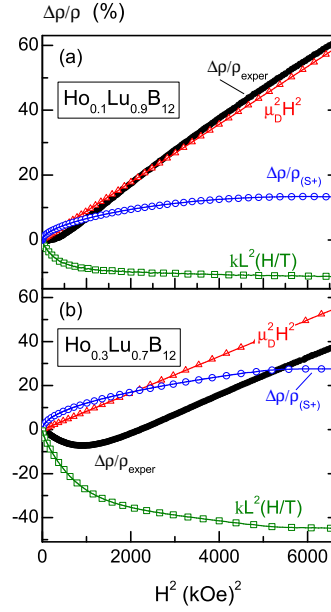


Figure 12. Two examples of MR analysis with contribution separation for (a) $\text{Ho}_{0.1}\text{Lu}_{0.9}\text{B}_{12}$ and (b) $\text{Ho}_{0.3}\text{Lu}_{0.7}\text{B}_{12}$ compounds at $T_0=2$ K. Symbols: \bullet correspond to experimental data ($\Delta\rho/\rho_{\text{exper}}$), \triangle , \circ – to positive contributions: $\mu_D^2 H^2$ and $\Delta\rho/\rho_{(S+)}$ and \square – to the saturated magnetic component $kL^2(H/T)$, respectively.

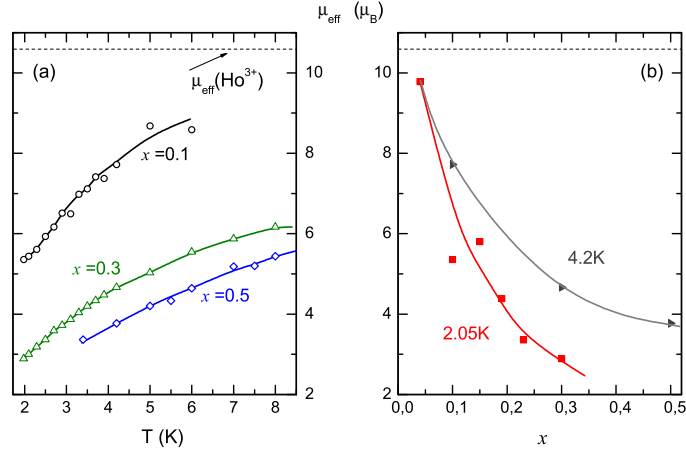


Figure 13. The temperature (a) and the concentration (b) dependences of effective magnetic moment μ_{eff} of $\text{Ho}_x\text{Lu}_{1-x}\text{B}_{12}$ with $x \leq 0.5$ (see the text). The dashed lines on both panels display the value of effective magnetic moment of Ho^{3+} ion.

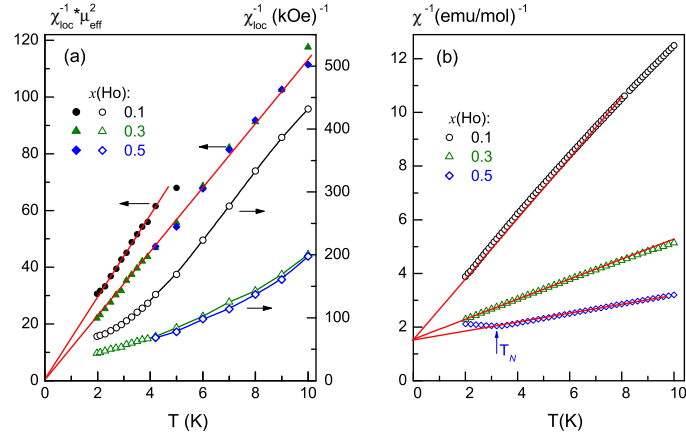


Figure 14. The temperature dependences of (a) the product $\chi_{\text{loc}}^{-1} \cdot \mu_{\text{eff}}^2$ (left axis) and the reciprocal local magnetic susceptibility $\chi_{\text{loc}}^{-1}(T)$ (right axis) and (b) reciprocal bulk magnetic susceptibility $\chi^{-1}(T)$ for $\text{Ho}_x\text{Lu}_{1-x}\text{B}_{12}$ solid solutions with $x = 0.1, 0.3$ and 0.5 . The solid straight lines show linear approximation.

fig.15. Following to the analysis of critical behavior of MR developed in [41], we have calculated also the critical exponent for the amplitude $D_{(AF)}$ of $\Delta\rho/\rho(AF)$ (see fig.15) in the framework of relation $D_{(AF)} \sim (1 - T/T_N)^{2\beta}$. The exponent $\beta = 0.37 \pm 0.02$ calculated for $\text{Ho}_{0.5}\text{Lu}_{0.5}\text{B}_{12}$ (see inset in fig.15) agrees very well with values $\beta = 0.36$ and 0.43 received previously in [41] for HoB_{12} , ErB_{12} and TmB_{12} , respectively. Within the framework of Yosida model [54] (see eq.1) a critical behavior of magnetoresistance is expected in vicinity of T_N , and exponents for MR (η) and for local magnetization (β) should be connected by relation $\eta = 2\beta$. The critical exponent $\beta = 0.37$ obtained here for $M_{loc} \sim (-\Delta\rho/\rho)^{1/2}$ is close to values $\beta = 0.335 \pm 0.005$ and $\beta = 0.385 \pm 0.01$ previously observed in magnetization studies of MnF_2 and RbMnF_3 antiferromagnets [55, 56]. In case of a three-dimensional Heisenberg model the critical exponent of magnetization calculated by expanding into series has a value of $\beta = 0.38 \pm 0.03$, whereas the critical exponent for the three-dimensional Ising model is $\beta = 0.312 \pm 0.005$ [57]. Therefore, the value of $\beta = 0.37$ obtained in this study for the $\text{Ho}_{0.5}\text{Lu}_{0.5}\text{B}_{12}$ magnet is physically justified and, according to our opinion, it can serve as an additional argument in favor of applicability of the spin-polaron approach used here to describe the magnetoresistance of the $\text{Ho}_x\text{Lu}_{1-x}\text{B}_{12}$ antiferromagnets. It is also worth to note that the temperature dependence of both the amplitude I_{AF} and the width Δ_{AF} of magnetic Bragg maxima for the antiferromagnetic phase of parent HoB_{12} compound was recently investigated in [58] using neutron diffraction technique. It was revealed that in vicinity of T_N the parameters I_{AF} and Δ_{AF} are characterized by a critical behavior with exponents $\beta \approx \gamma \approx 1/3$, which are also in accordance with the critical exponent $\beta \approx 0.37$ received here for $\text{Ho}_{0.5}\text{Lu}_{0.5}\text{B}_{12}$.

To identify precisely the magnetic phase transitions both between AF and P phases and inside the AF state, a numerical differentiation analysis of resistivity curves has been carried out, and features of derivatives $d\rho/dH$ (see figs.16a,b) were used to construct the H - T magnetic phase diagram of $\text{Ho}_{0.5}\text{Lu}_{0.5}\text{B}_{12}$ (see fig.16c). The received H - T diagram presented in Fig.16c for $\text{Ho}_{0.5}\text{Lu}_{0.5}\text{B}_{12}$ is similar to that observed in [41, 48] for parent antiferromagnet HoB_{12} with a higher Neel temperature $T_N \approx 7.4$ K. The high accuracy of resistivity measurements allowed us also to analyze and classify the MR components observed in the AF_1 and AF_2 phases of the solid solution with $x=0.5$. Indeed, the analysis of linear fragments of resistivity derivatives (fig.16b) allows to describe the magnetoresistance of $\text{Ho}_{0.5}\text{Lu}_{0.5}\text{B}_{12}$ through the relationship

$$\Delta\rho/\rho(H, T_0) = -B_{1,2}(T_0)H^2 + A_{1,2}(T_0)H + C. \quad (2)$$

Eq.2 provides us with a good quality approximation of the MR results both below (phase AF_1 , B_1 and A_1 coefficients in Eq.2) and above (phase AF_2 , B_2 and A_2 coefficients in Eq.2) the $T_C(H)$ phase boundary (linear fits for $d\rho/dH$ are shown in fig.16b). The calculated temperature dependences of coefficients $B_{1,2}(T_0)$ and $A_{1,2}(T_0)$ are presented in figs.17a,b, respectively. As can be seen from figs.16b and 17b, simultaneously with the negative quadratic term $\Delta\rho/\rho(-) = -B_{1,2}(T_0)H^2$ a linear positive component $A_{1,2}(T_0)H$ of magnetoresistance appears in the vicinity of T_N in the AF phase of $\text{Ho}_{0.5}\text{Lu}_{0.5}\text{B}_{12}$, and coefficients A and B change jump-wise in moderate magnetic field 15-25 kOe between (A_1, B_1) and (A_2, B_2) values during the AF_1 - AF_2 phase transition observed at T_C . Following the arguments presented previously in [41, 52, 53], the appearance of a linear positive contribution to MR in the antiferromagnetic phase should be attributed to scattering of charge carriers on spin density waves (SDW). In particular, in case of metallic chromium which is the most known 3D itinerant antiferromagnet with SDW (having an incommensurate magnetic structure), the amplitude of linear positive magnetoresistance reaches 180% at magnetic field of $H=12$ kOe [59]. Similar effects have been found recently [47] in the magnetoresistance of $\text{Tm}_{1-x}\text{Yb}_x\text{B}_{12}$ antiferromagnets with the same modulated incommensurate magnetic structure ($q = (1/2 \pm \delta, 1/2 \pm \delta, 1/2 \pm \delta)$ with $\delta = 0.035$) as in HoB_{12} [58, 60]. Thus,

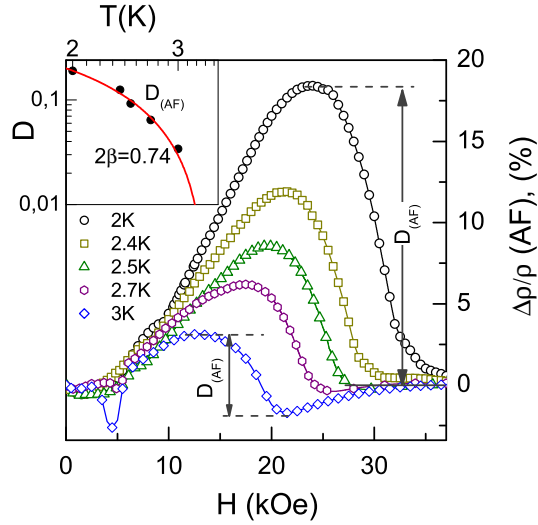


Figure 15. The field dependences of $\Delta\rho/\rho(\text{AF})$ term of magnetoresistance of $\text{Ho}_{0.5}\text{Lu}_{0.5}\text{B}_{12}$. D_{AF} designate the amplitude of the MR component. The inset shows the result of critical exponent analysis $D_{\text{AF}} \sim (1 - T/T_N)^{-2\beta}$ (see the text).

according to our analysis, the $\text{AF}_1\text{--AF}_2$ transition observed in $\text{Ho}_{0.5}\text{Lu}_{0.5}\text{B}_{12}$ at T_C (fig.16c) may be considered as a modification of the spin-density-wave structure, which manifests itself both in (i) changes of the charge carrier scattering on magnetic nanodomains consisting from interconnected Ho^{3+} ions (expressed by the negative quadratic Langevin type MR component) and (ii) through the increase of the SDW amplitude with increasing magnetic field, resulting to enhancement of charge carrier scattering on SDW (expressed through the linear positive MR term). We note that the stabilization and enhancement of SDW in external magnetic field is predicted previously [61, 62]. However, at the same time, to our best knowledge, no theoretical description of charge transport in the presence of an external magnetic field in itinerant magnets with incommensurate SDW structure is available to date, which restricts the possibility of a more detailed microscopic analysis of the positive magnetoresistance effect in the rare earth dodecaborides.

To summarize the results of this section, we want to discuss below shortly the mechanisms responsible for the emergence of various magnetic phases in the AF state of $\text{Ho}_x\text{Lu}_{1-x}\text{B}_{12}$ compounds having a simple face centered cubic crystal structure (fig.1a-c). To explain the nature of intermediate phases in the AF state of HoB_{12} , authors of [46] proposed a model that considers frustration effects in the *fcc* lattice of RB_{12} . However, when taking into account (i) the loosely bounded state of rare earth ions in the dodecaboride matrix, (ii) the transition into the cage-glass state of RB_{12} at liquid nitrogen temperatures [39], and (iii) the appearance of disorder in the arrangement of rare earth ions (random off-site location of Ho^{3+} -ions inside the B_{24} truncated cubooctahedron) resulting to formation of magnetic nanosize clusters in studied compounds, it becomes possible to explain the numerous phase transformations in the AF state as a function of temperature and external magnetic field. Indeed, positional disorder in the arrangement of Ho^{3+} ions in B_{24} truncated cubooctahedrons leads to a significant dispersion of exchange constants (through indirect exchange, RKKY mechanism). Strong local $4f\text{--}5d$ spin fluctuations then cause the appearance of an extra factor – the polarization of $5d$ conduction

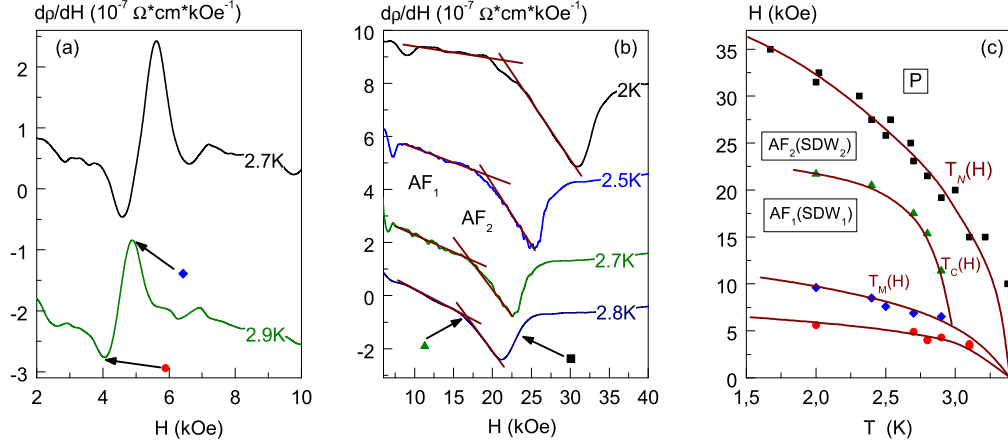


Figure 16. (a-b) Results of the numerical differentiation of resistivity $d\rho/dH$ in AF state of $\text{Ho}_{0.5}\text{Lu}_{0.5}\text{B}_{12}$ compound. The arrows indicate the magnetic phase transitions. (c) H - T magnetic phase diagram of $\text{Ho}_{0.5}\text{Lu}_{0.5}\text{B}_{12}$, reconstructed from MR data. Abbreviations: P – paramagnetic state, AF_{1,2} (SDW_{1,2}) – antiferromagnetic spin-density wave phases.

band states (the spin-polaron effect). Moreover, the transition from paramagnetic to AF phase is accompanied by the appearance of induced spin polarization (formation of ferrons, according to the terminology used in [63, 64]) and by stabilization of these SDW antinodes in the RB_{12} matrix. The spin-polarized $5d$ -component of the magnetic structure (ferrons) is from one side very sensitive to external magnetic field, and, from another side, the applied field suppresses $4f$ – $5d$ spin fluctuations by destroying the spin-flip scattering process. Thus, the complex H - T phase diagram of $\text{Ho}_x\text{Lu}_{1-x}\text{B}_{12}$ magnets may be explained in terms of the formation of a combined magnetically ordered state of localized $4f$ moments of Ho^{3+} -ions in combination with spin polarized local areas of the $5d$ states – ferrons involved in the formation of a spin density waves. The presence of the spin polarization was confirmed for HoB_{12} in [46] where ferromagnetic component of the order parameter was found in the magnetic neutron diffraction patterns. Moreover, even harmonics and hysteresis of the Hall resistance were detected in the range $20 \text{ kOe} < H < 60 \text{ kOe}$ for HoB_{12} and it was attributed to charge carriers scattering on SDW [48].

V. Conclusions

We have studied in detail the transverse magnetoresistance of the model metallic system with loosely bound state of rare earth magnetic ions (Ho^{3+}) embedded in large size cavities (B_{24} truncated cubooctahedrons) of the boron sublattice of $\text{Ho}_x\text{Lu}_{1-x}\text{B}_{12}$ substitutional solid solutions. It was shown that positive as well as negative magnetoresistance can be observed in measurements of single crystals of these cage-glass materials. The nMR component which appears in the paramagnetic state of these magnetic metals, may be explained in terms of charge carriers scattering on nanosize clusters of Ho ions with AF exchange and short range AF order inside these domains. An enhancement of the nMR effect is observed in concentrated Ho-based dodecaborides in the vicinity of Neel temperature, and the Yosida type relation $-\Delta\rho/\rho \sim M^2$

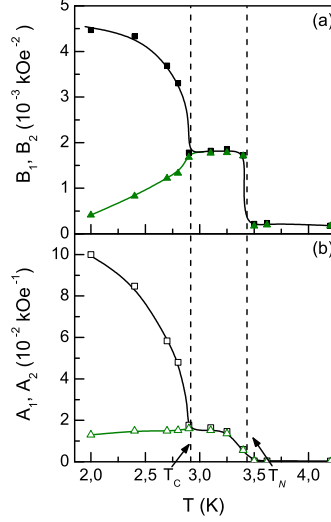


Figure 17. The temperature dependences of the amplitudes of (a) negative quadratic term ($B_{1,2}$) and (b) linear positive ($A_{1,2}$) component in magnetoresistance of $\text{Ho}_{0.5}\text{Lu}_{0.5}\text{B}_{12}$ compound (see the Eq.2).

between magnetoresistance and magnetization is found to provide an adequate description of this term if a Langevin type behavior of magnetization is present. Moreover, a reduction of effective values of Ho-ion magnetic moments in the range $3-9\mu_B$ was found to develop both with temperature lowering and under increase of holmium content. It was shown in the MR analysis that the positive quadratic term $\Delta\rho/\rho_{(m+)}=\mu_D^2 H^2$ dominates for all solid solutions of $\text{Ho}_x\text{Lu}_{1-x}\text{B}_{12}$ at intermediate temperatures 20-120 K in strong magnetic fields, allowing to estimate the exponential behavior of drift mobility of charge carriers $\mu_D \sim T^{-\alpha}$ ($\alpha=1.3-1.7$). In the AF state an additional positive linear MR contribution $\Delta\rho/\rho \sim A(T)H$ was found and it was attributed to charge carriers scattering on SDW in the incommensurate magnetic structure of these unusual antiferromagnets. In accordance with magnetic field induced modification of the AF state which has been observed recently in neutron scattering studies of HoB_{12} [46] we argue in favor of a SDW₁-SDW₂ magnetic phase transition in $\text{Ho}_{0.5}\text{Lu}_{0.5}\text{B}_{12}$ in external fields of 10–25 kOe. The presented comprehensive MR analysis allows to reconstruct the H - T magnetic phase diagram of $\text{Ho}_{0.5}\text{Lu}_{0.5}\text{B}_{12}$, and provide arguments in favor of a superposition of two components, the $4f$ (based on Ho^{3+} localized moments) and the itinerant $5d$ (based on SDW) parts, which form the complex magnetic structure of $\text{Ho}_x\text{Lu}_{1-x}\text{B}_{12}$ antiferromagnets.

ACKNOWLEDGMENTS

We would like to thank V.V. Moshchalkov, A.V. Kuznetsov, G.E. Grechnev, J. Stankiewicz and K. Siemensmeyer for numerous helpful discussions. This study was supported by the Branch of Physical Sciences of the Russian Academy of Sciences within the program "Strongly Correlated Electrons in Semiconductors, Metals, Superconductors, and Magnetic Materials", Young scientists Grant of RF President No. MK-6427.2014.2, and Slovak Scientific Grant Agencies VEGA-2/0106/13, APVV-0132-11.

References

- [1] W. Thomson, *Proc. Royal Soc. London* **8**, 546 (1856-1857).
- [2] C. M. Varma, *Phys. Rev. B* **54**, 7328 (1996).
- [3] P. Majumdar, P. Littlewood, *Phys. Rev. Lett.* **81**, 1314 (1998).
- [4] A. A. Abrikosov, *Phys. Rev. B* **58**, 2788 (1998).
- [5] M. M. Parish and P. B. Littlewood, *Phys. Rev. B* **72**, 094417 (2005).
- [6] J. Hu, M. M. Parish and T. F. Rosenbaum, *Phys. Rev. B* **75**, 214203 (2007).
- [7] V. B. Shenoy, T. Gupta, H. R. Krishnamurthy and T. V. Ramakrishnan, *Phys. Rev. B* **80**, 125121 (2009).
- [8] D. I. Golosov, *Phys. Rev. Lett.* **104**, 207207 (2010).
- [9] N. V. Kozlova, N. Mori, O. Makarovskiy, L. Eaves, Q. D. Zhuang, A. Krier and A. Patane, *Nat. Commun.* **3**, 1097 (2012).
- [10] N. J. Harmon and M. E. Flatte, *Phys. Rev. Lett.* **108**, 186602 (2012).
- [11] F. L. Bloom, W. Wagemans, M. Kemerink, and B. Koopmans, *Phys. Rev. Lett.* **99**, 257201 (2007).
- [12] Yu. Wang and J. J. Santiago-Avilés, *Appl. Phys.* **89**, 123119 (2006).
- [13] B. R. Matis, F. A. Bulat, A. L. Friedman, B. H. Houston, J. W. Baldwin, *Phys. Rev. B* **85**, 195437 (2012).
- [14] X. Hong, S.-H. Cheng, C. Herding, J. Zhu, *Phys. Rev. B* **83**, 085410 (2011).
- [15] F. Hellman, M. Q. Tran, A. E. Gebala, E. M. Wilcox, R. C. Dynes, *Phys. Rev. Lett.* **77**, 4652 (1996).
- [16] S. D. Ganichev, H. Ketterl, W. Prettl, I. A. Merkulov, V. I. Perel, I. N. Vassievich, A. V. Malyshev, *Phys. Rev. B* **63**, 201204(R) (2001).
- [17] T. A. Dauzhenka, V. K. Ksenevich, I. A. Bashmakov, J. Galibert, *Phys. Rev. B* **83**, 165309 (2011).
- [18] R. Xu, A. Husmann, T. F. Rosenbaum, M.-L. Saboungi, J. E. Enderby, P. B. Littlewood, *Nature (London)* **390**, 57 (1997).
- [19] A. Husmann, J. B. Betts, G. S. Boebinger, A. Migliori, T. F. Rosenbaum, M.-L. Saboungi, *Nature (London)* **417**, 421 (2002).
- [20] T. Thio, S. A. Solin, J. W. Bennett, D. R. Hines, M. Kawano, N. Oda, M. Sano, *Phys. Rev. B* **57**, 12239 (1998).
- [21] P. Allia, M. Coisson, V. Selvaggini, P. Tiberto, F. Vinai, *J. Magn. Magn. Matt.* **262**, 39 (2003).
- [22] G. A. Prinz, *Science* **282**, 1660 (1998).

- [23] S. Jin, T. H. Tiefel, M. McCormack, R. A. Fastnacht, R. Ramesh, L. H. Chen, *Science* **264**, 413 (1994).
- [24] E. Dagotto, T. Hotta, A. Moreo, *Phys. Rep.* **344**, 1 (2001).
- [25] G. Briceño, H. Chang, X. Sun, P. G. Shultz and X.-D. Xiang, *Science* **270**, 273 (1995).
- [26] K.-I. Kobayashi, T. Kimura, H. Sawada, K. Terakura and Y. Tokura, *Nature (London)* **395**, 677 (1998).
- [27] S. Süllo, I. Prasad, S. Bogdanovich, M.C. Aronson, J.L. Sarrao and Z. Fisk, *J. Appl. Phys.* **87**, 5591 (2000).
- [28] N. Y. Shimakawa, Y. Kubo and T. Manako, *Nature (London)* **379**, 53 (1996).
- [29] V. A. Gavrichkov, N. B. Ivanova, S. G. Ovchinnikov, T. G. Aminov, A. D. Balaev, G. G. Shabunina, V. K. Chernov, M. V. Petukhov, *Phys. Solid State* **41**, 1652 (1999).
- [30] S. Weber, P. Lunkenheimer, R. Fichtl, J. Hemberger, V. Tsurkan, A. Loidl, *Phys. Rev. Lett.* **96**, 157202 (2006).
- [31] S. M. Watts, S. Wirth, S. von Molnar, A. Barry and J.M.D. Coey, *Phys. Rev. B* **61**, 9621 (2000).
- [32] H. Li, Y. Xiao, B. Schmitz, J. Persson, W. Schmidt, P. Meuffels, G. Roth, Th. Brückel, *Sci. Rep.* **2**, 750 (2012).
- [33] S. V. Demishev, V. V. Glushkov, I. I. Lobanova, M. A. Anisimov, V. Yu. Ivanov, T. V. Ishchenko, M. S. Karasev, N. A. Samarin, N. E. Sluchanko, V. M. Zimin, A. V. Semeno, *Phys. Rev. B* **85**, 045131 (2012).
- [34] N. E. Sluchanko, A. V. Bogach, V. V. Glushkov, S. V. Demishev, V. Yu. Ivanov, M. I. Ignatov, A. V. Kuznetsov, N. A. Samarin, A. V. Semeno, and N. Yu. Shitsevalova, *JETP* **104**, 120 (2007).
- [35] A. V. Bogach, G. S. Burkhanov, O. D. Chistyakov, V. V. Glushkov, S. V. Demishev, N. A. Samarin, Yu. B. Paderno, N. Yu. Shitsevalova, N. E. Sluchanko, *Physica B* **378-380**, 769 (2006).
- [36] J. Y. Chan, S. Kauzlarich, P. Klavins, R. N. Shelton, D. J. Webb, *Phys. Rev. B* **57**, R8103(R) (1998).
- [37] M. B. Salamon, P. Lin, S. H. Chun, *Phys. Rev. Lett.* **88**, 197203 (2002).
- [38] N. E. Sluchanko, A. N. Azarevich, A. V. Bogach, V. V. Glushkov, S. V. Demishev, A. V. Kuznetsov, K. S. Lyubshov, V. B. Filippov, N. Yu. Shitsevalova, *JETP* **111**, 279 (2010).
- [39] N. E. Sluchanko, A. N. Azarevich, A. V. Bogach, I. I. Vlasov, V. V. Glushkov, S. V. Demishev, A. A. Maksimov, I. I. Tartakovskii, E. V. Filatov, K. Flachbart, S. Gabáni, V. B. Filippov, N. Yu. Shitsevalova, V. V. Moshchalkov, *JETP* **113**, 468 (2011).
- [40] N. Sluchanko, S. Gavrilkin, K. Mitsen, A. Kuznetsov, I. Sannikov, V. Glushkov, S. Demishev, A. Azarevich, A. Bogach, A. Lyashenko, A. Dukhnenko, V. Filippov, S. Gabáni, K. Flachbart, J. Vanacken, Gufei Zhang, V. Moshchalkov, *J. Supercond Nov. Magn.* **26**, 1663 (2013).

- [41] N. E. Sluchanko, A. V. Bogach, V. V. Glushkov, S. V. Demishev, N. A. Samarin, D. N. Sluchanko, A. V. Dukhnenko, A. V. Levchenko, *JETP* **108**, 668 (2009).
- [42] S. Gabáni, I. Bat'ko, M. Bat'ková, K. Flachbart, E. Gažo, M. Reiffers, N. Shitsevalova, K. Siemensmeyer, N. Sluchanko, *Solid State Sciences* **14**, 1722 (2012).
- [43] S. Gabáni, E. Gažo, G. Pristáš, I. Takáčová, K. Flachbart, N. Shitsevalova, K. Siemensmeyer, N. Sluchanko, *J. Korean Phys. Soc.* **62**, 1514 (2013).
- [44] Yu. Paderno, V. Filippov, and N. Shitsevalova, in *Boron-Rich Solids*, ed. by D. Emin and T. L. Aselage (American Institute of Physics, Albuquerque, NM, United States, 1991), *AIP Conf. Proc.* **230**, 460 (1991).
- [45] D. L. Strandburg, S. Legvold, F. H. Spedding, *Phys. Rev.* **127**, 2046 (1962).
- [46] K. Siemensmeyer, K. Babicht, Th. Lonkai, S. Mat'aš, S. Gabáni, N. Shitsevalova, E. Wulf, K. Flachbart, *J. Low Temp. Phys.* **146**, 581 (2007).
- [47] N. E. Sluchanko, A. N. Azarevich, A. V. Bogach, V. V. Glushkov, S. V. Demishev, A. V. Levchenko, V. B. Filippov, N. Yu. Shitsevalova, *JETP* **116**, 866 (2013).
- [48] N. E. Sluchanko, D. N. Sluchanko, V. V. Glushkov, S. V. Demishev, N. A. Samarin, N. Yu. Shitsevalova, *JETP Lett.* **86**, 604 (2008).
- [49] P. Wagner, I. Gordon, L. Trappeniers, J. Vanacken, F. Herlach, V. V. Moshchalkov, Y. Bruynseraede, *Phys. Rev. Lett.* **81**, 3980 (1998).
- [50] N. E. Sluchanko, A. V. Bogach, G. S. Burkhanov, O. D. Chistyakov, V. V. Glushkov, S. V. Demishev, N. A. Samarin, D. N. Sluchanko, *Physica B* **359-361C**, 308 (2005).
- [51] A. V. Bogach, G. S. Burkhanov, O. D. Chistyakov, V. V. Glushkov, S. V. Demishev, N. A. Samarin, Yu. B. Paderno, N. Yu. Shitsevalova, N. E. Sluchanko, *Physica B* **378-380**, 769 (2006).
- [52] M. A. Anisimov, A. V. Bogach, V. V. Glushkov, S. V. Demishev, N. A. Samarin, V. B. Filipov, N. Yu. Shitsevalova, A. V. Kuznetsov, N. E. Sluchanko, *JETP* **109**, 815 (2009).
- [53] M. A. Anisimov, A. V. Bogach, V. V. Glushkov, S. V. Demishev, N. A. Samarin, N. Yu. Shitsevalova, A. V. Levchenko, V. B. Filipov, A. V. Kuznetsov, N. E. Sluchanko, *J. Phys. Conf. Ser.* **400**, 032003 (2012).
- [54] K. Yosida, *Phys. Rev.* **107**, 396 (1957).
- [55] P. Heller, *Phys. Rev.* **146**, 403 (1966).
- [56] A. Sabba Stefanescu and P.-J. Becker, *J. Phys. C: Solid State Phys.* **14**, L737 (1981).
- [57] S. Ma, *Modern Theory of Critical Phenomena* (Benjamin, Reading, MA), United States (1976).
- [58] K. Flachbart, P. Alekseev, G. Grechnev, N. Shitsevalova, K. Siemensmeyer, N. Sluchanko, and O. Zogal, *In Rare Earths: Research and Applications* ed. K.N. Delfrey (Nova Science, Hauppauge, NY) **Ch.2**, 79-125 (2008).
- [59] S. Arajs and G. R. Dunmyre, *J. Appl. Phys.* **36**, 3555 (1965).

- [60] K. Siemensmeyer, K. Flachbart, S. Gabáni, S. Mat'aš, Y. Paderno, and N. Shitsevalova, *J. Solid State Chem.* **179**, 2748 (2006).
- [61] T. Sasaki, A. Lebed', T. Fukase, and N. Toyota, *Phys. Rev. B: Condens. Matter* **54**, 12969 (1996).
- [62] G. Montambaux, *Phys. Rev. B: Condens. Matter* **38**, 4788 (1988).
- [63] E. L. Nagaev, *JETP Lett.* **6** (1), 18 (1967).
- [64] M. Yu. Kagan, K. I. Kugel, and D. I. Khomskii, *JETP* **93** (2), 415 (2001).

SUPPLEMENTARY INFORMATION

internet files:

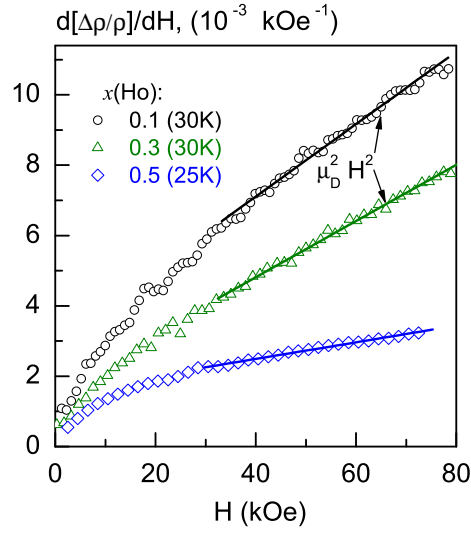


Figure SI.1. The field dependences of derivatives of MR $d[\Delta\rho/\rho]/dH$ for solid solutions $\text{Ho}_x\text{Lu}_{1-x}\text{B}_{12}$ with $x=0.1, 0.3$ and 0.5 . The positive quadratic term's approximation is illustrated by solid lines.

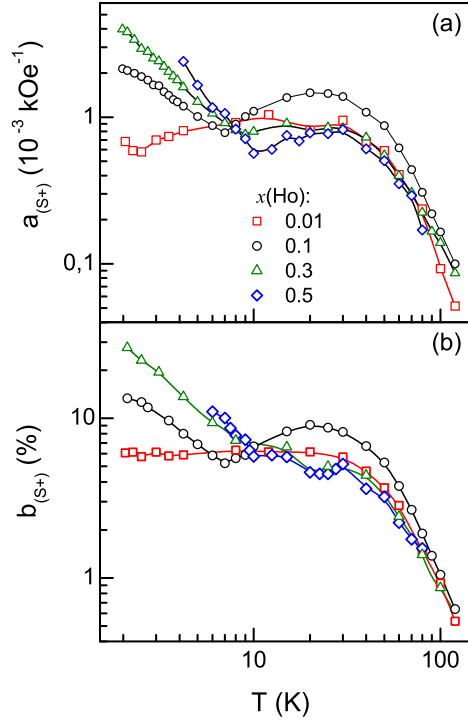


Figure SI.2. The temperature dependences of the amplitudes of (a) linear positive term $\sim a_{(S+)}H$ and (b) saturated component $b_{(S+)}$ of magnetoresistance for solid solutions $\text{Ho}_x\text{Lu}_{1-x}\text{B}_{12}$ with $x=0.01, 0.1, 0.3$ and 0.5 (see the text).